Survey Paper

DIGITAL TWIN BASED LIGHTWEIGHTING OF ROBOT UNMANNED GROUND VEHICLES

UDC (621.391:004.934)

Milan Banić[1], Miloš Simonović[2], Lazar Stojanović[2], Damjan Rangelov[1], Aleksandar Miltenović[1], Marko Perić[1]

[1]University of Niš, Faculty of Mechanical Engineering, Department of Machine Design, Development and Engineering, Republic of Serbia
[2]University of Niš, Faculty of Mechanical Engineering, Department of Mechatronics and Control, Republic of Serbia

Abstract. *Battery powered outdoor robot Unmanned Ground Vehicles (UGV) should have minimal mass for designed payload capacity to facilitate their movement on rough terrain and increase their autonomy. On the other hand, stiffness and strength of their mechanical components should be sufficient to sustain operational loads. The paper presents the case study of robot UGV lightweighting based on UGV digital twin data. The process of creation of robot UGV digital twin is described, as well as the type and quantity of data acquired from robot sensors. Based on the data from the digital twin of the robot about operational loads, the worst operational load cases were identified and the structural analysis of the robot chassis for noted load cases was performed. The results of the analysis were used in the topology optimization of the robot UGV mechanical components with a goal to satisfy design requirements and reduce the robot mass. By application of noted procedure the mass reduction of approximately 17 % was achieved.*

Key words: *Robot unmanned ground vehicle, Digital twin, Lightweight design, Static structural analysis, Topology optimization*

1. INTRODUCTION

Outdoor robot UGV move over the rough terrain, and it is necessary to ensure satisfactory strength and stiffness of the robot mechanical components against impacts, bending, twisting during movement and changes in the direction of movement. The geometry of the robot

during operation must not be compromised, thus deformation of the chassis must be as low as possible to ensure the robot functionality, as well as the sensors/actuators positioning and accuracy of sensor readings. Furthermore, the robot mass must be as low as possible to improve the robot autonomy, lower the dynamic forces and decrease the ground pressure in order to increase maneuverability. Lowering of robot mass for a same strength and stiffness also allows to increase the usable payload. The conflict of requirements regarding strength and stiffness and keeping the robot mass as low as possible can be solved by principles of lightweight design. The lightweight design is a development strategy, which aims to realize a required function with a system minimized mass under predefined boundary conditions [1]. The lightweight design can be achieved in many ways that include material substitution, design elements thickness reduction, and change of shape of the parts, or elimination of parts that do not contribute significantly to stiffness, without sacrificing the overall structural integrity or functionality [2]. But to perform the lightweighting procedure, operational loads must be known. Determining the operational loads that an outdoor robot UGV may experience can be a complex and challenging task, as it requires considering a wide range of factors that can impact the loads experienced by the robot. As by its nature the digital twin contains data about operational loads, the noted fact can be used in the system lightweighting [3].

The Digital Twin (DT) is the virtual representation of a physical object/system across its full life-cycle using real-time operational data and other sources to enable understanding, learning, reasoning, and dynamical recalibration for improved decision making [4]. Although DT was introduced as a concept during the 1960s by NASA, it is officially recognized in 2002 at the University of Michigan. Since then, DT is gaining in popularity as one of the most cost-effective technologies in real applications [5]. Using data derived from Internet of Things (IoT) sensor technologies that are attached or embedded in a physical object the digital twin provides an opportunity to transfer the physical objects/system to a virtual objects/system, so that there is a possibility of creating virtual representations of products, or simulate of various operational processes, manipulate and monitor them [6]. DT can have multiple maturity levels based on the degree of communication between digital and the physical domain, or according to the communication direction and intelligent data processing [7].

Goraj [8] predicted a fatigue lifetime based on an one-step load spectrum. Time-dependent normal and shear stress components were estimated using a high-fidelity digital twin built in Siemens PLM Nx Nastran. The author considered all structural and thermal loads identified by sensor data and estimated the equivalent cyclic degree of utilization and a safety margin against the slip of a press-fitted shaft to rotor hub connection. Kokonen et all [9] used the digital twin for collecting information of manufacturing the quality deviation in the case of welded structures and for the prediction of the individual remaining fatigue lives. The authors considered that design goal was minimizing the mass of the structure as a process of optimization, while the required fatigue life is defined as a constraint. Ryll et all [10] demonstrate the potential of the digital twin technology in a hybrid lightweight structure by realizing the demonstrator for creating a table size of aluminum profiles. Rupfle el all [11] used a digital twin for real-time analysis of load and displacement calculation of large-scale onshore wind turbines. Based on a digital twin data the "Message Queuing Telemetry Transport" (MQTT) transmission protocol was chosen for the lightweight design of constrained services. Zhang et all [12] optimized the wall-climbing robot system by implementing multiple sensors integration for magnetic particle testing. They established a high-quality detection that is based on the collected sensor information and a multi-degree of freedom component collaborative flexible detection.

Digital twin approach thus is providing a good basis of data for the lightweight design of products. Combining real-data information with detailed data about the flight missions of the whole aircraft fleet gives better picture about the real use and requirements for lightweight structure [13, 14, 15]. Herlitzius [16] estimated that tractors and self-propelled machines today realize a power-to-weight ratio of 45 kg/kW (±15 %). Potential of lightweight design in these cases is almost halved for the same power.

The paper presents the lightweighting procedure of robot UGV based on robot digital twin data about operational loads. The process of creation of robot digital twin is described, as well as the data acquisition from robot sensors. Based on the data from the digital twin of the robot, the worst load cases were identified and the structural analysis of the robot mechanical components for noted load cases was performed. The results of the analysis were used in the topology optimization of the robot mechanical components with a goal to satisfy design requirements and reduce the robot mass.

2. THE LIGHTWEIGHTING STUDY OBJECT

The object of the lightweighting case study is a TRL6 (TRL – Technology Readiness Level) prototype of a battery powered robot UGV developed by the company Coming Computer Engineering and the Faculty of Mechanical Engineering of University of Niš. The robot, branded as Agriculture Autonomous Robot (AgAR), is developed for indoor and outdoor tasks and designed with precision agriculture in mind. Equipped with ROS based software that enables remote control, moving along predefined paths, and autonomous movement, AgAR represents a multipurpose robotic UGV platform which can accommodate extensive variety of payloads customized to meet precision agriculture needs. Due to the rugged design and high torque drive train AgAR can cover rough terrain with high gradient slopes even with large payloads.
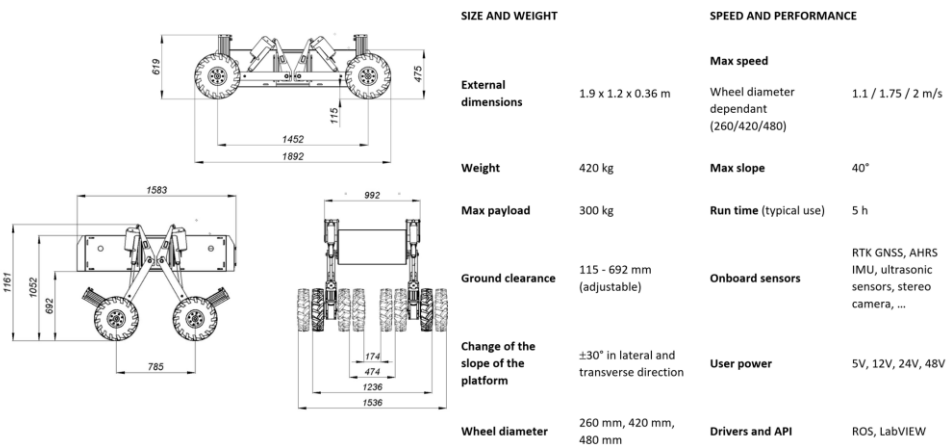
AgAR robotic platform consists of four main subassemblies, subassembly of the main body, main body enclosure, mechanism for the change of clearance from the ground, and a subassembly of the drive train as shown on Figure 1.
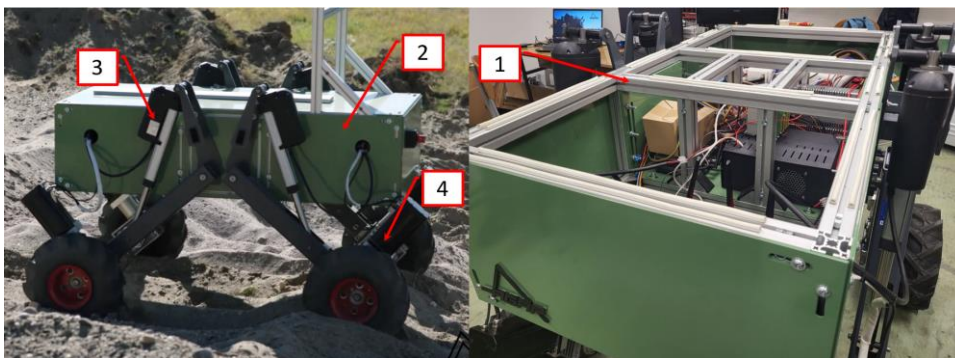
Fig. 1 3D model of AgAR with marked subassemblies

The subassembly (1, Figure 1) of the main body is made of standard aluminum profiles for easier assembly and disassembly and protected with a sheet metal enclosure (2, Figure 1). To

increase the stiffness of the main body, in every corner of the main body there is a reinforcement in the form of steel plates. The subassembly of the mechanism for changing the clearance from the ground of the main body (3, Figure 1) is designed as a four bar mechanism where the connecting rod is expandable. The mechanism rocker is a square tube, and the mechanism position change is achieved by the extension of the rod of electric linear actuator which acts as a connecting rod. As there are four mechanisms for changing the clearance from the ground of the main body, it is possible to change the height of the main body from the ground i.e. clearance of the robot, as well to adjust the inclination of the main body in lateral and longitudinal directions. The subassembly of the drive train (4, Figure 1) consists of 1 kW BLDC motor, worm gearbox with reduction ratio 1:40 and a wheel with a pneumatic tire connected to the worm gearbox output shaft via a wheel hub. The motor and worm gearbox are connected by an elastic coupling which is transferring the torque from the motor to the worm gearbox. The connection between subassemblies is designed as separable, with bolted connections. Such robot design allows for easy changes to the universal robotic platform, satisfying the requirements related to modularity and universality. The overall AgAR overall dimensions and its technical specification are shown on Figure 2. The total mass of the robot with all components is 420 kg, while the mass of the robot mechanical components is 340 kg.

| SIZE AND WEIGHT		SPEED AND PERFORMANCE	
		Max speed	
External dimensions	1.9 x 1.2 x 0.36 m	Wheel diameter dependant (260/420/480)	1.1 / 1.75 / 2 m/s
Weight	420 kg	Max slope	40°
Max payload	300 kg	Run time (typical use)	5 h
Ground clearance	115 - 692 mm (adjustable)	Onboard sensors	RTK GNSS, AHRS IMU, ultrasonic sensors, stereo camera, ...
Change of the slope of the platform	±30° in lateral and transverse direction	User power	5V, 12V, 24V, 48V
Wheel diameter	260 mm, 420 mm, 480 mm	Drivers and API	ROS, LabVIEW

Fig. 2 AgAR dimensions and technical specification

The AgAR is equipped with an extensive set of sensors which continuously acquire data during its operation as shown on Figure 3. The robot position is determined by the fusion of data from the Real Time Kinematic (RTK) GNSS system and Attitude and Heading Reference system (AHRS) Inertial Measurement Unit (IMU). The AHRS IMU also acquires data about the acceleration in all three directions, as well as roll, pitch, yaw and angular acceleration of the robot main body. The environment perception is enabled by 3D LiDAR, stereo camera, RGB camera and four Ultrasonic Sensors (US). The BLDC motor controllers also gather data about the motor RPM, motor voltage (U), current (I) and motor and controller temperature (T), as well as other data significant for the robot operation. The data about battery operational parameters (U, I, T and State of Charge – SoC) are also acquired from the smart Battery Management System (BMS).

**Fig. 3** AgAR sensor set and data gathered by a digital twin
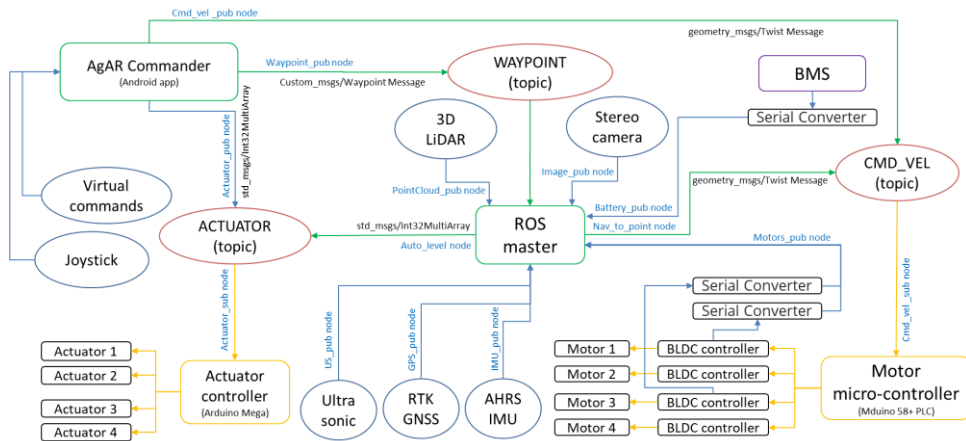
Fig. 4 AgAR sensor set and data gathered by a digital twin

All of above-mentioned sensor data are acquired stored both locally and in a cloud to form an AgAR smart monitor digital twin according to the control architecture shown on Figure 4. The sensor data are acquired locally, stored, organized and structured on ROS master (Industrial PC), where they are processed and control algorithms are applied. The robot has three operational modes – teleoperation, GPS navigation and autonomous movement. In each of the operational modes, the sensor data is acquired at 25 Hz. Furthermore, the most significant data is visualized on the AgAR Android app – AgAR Commander in real-time.

3. LIGHTWEIGHTING METHOD

The lightweighting procedure was performed based on the assumption that the robot mechanical components must have sufficient strength and stiffness to sustain the worst-case operational loads. The worst-case operational loads were identified by the analysis of digital twin data, which was gathered during the validation of the TRL6 AgAR prototype against all the functional and technical requirements for all use cases defined and for a maximal AgAR payload. Two worst-case operational load cases were identified:

- during the change of direction of movement by a rotation around the central vertical axis i.e. during "tank" in place turning with maximal payload and with minimal clearance, and
- while climbing the curb on direct path of moving at full speed.
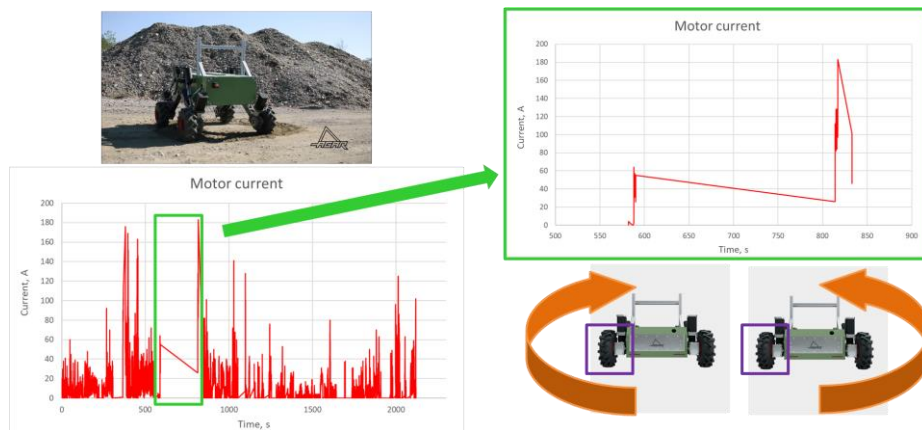
Fig. 5 Identification of worst-case load case scenario by motor current

The motor current during the movement of the robot can be seen on Figure 5. The peaks in the motor current diagram correspond to the "tank" turning. It was observed during testing that the maximal peaks occur while the robot is in minimal clearance from the ground configuration i.e. when the wheels have a maximal distance from vertical axis of rotation. Furthermore, from Figure 5, one can observe that the motor current while robot performs the "tank" turning is not the same on the motors on the left and right robot side – the motors on the left robot side during counter clock rotation have up to three times larger current than the motors on the right robot side. The same applies for clockwise rotation, as in that case the motors on the right have approximately three times larger current than the motors on the left robot side. As the motor current is directly proportional to the generated torque by a motor constant, it is straightforward to calculate the torque on wheels during the "tank" turning according to:

$$T = K \cdot I \cdot i \cdot \eta \tag{1}$$

where: T - torque on wheel, K - motor constant (0.142 Nm/A), I - motor current, i - worm gear transmission ratio (40) and η worm gear efficiency (0.7).
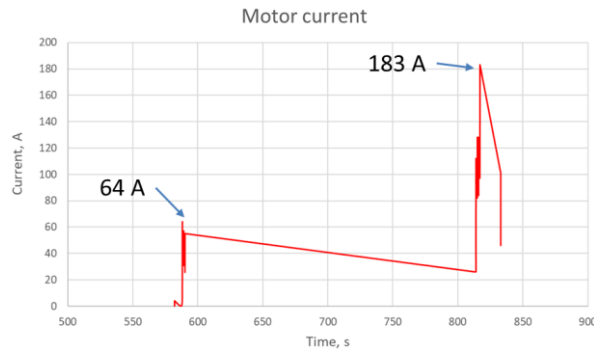
Fig. 6 Maximal values of motor current during "tank" robot rotation

Based on maximal values of motor current for the right and left robot side (183 and 64 A), as shown in Figure 6, by substituting the maximal values into equation 1, the maximal torques were calculated $T_{right} = 728$ Nm and $T_{left} = 254.5$ Nm.
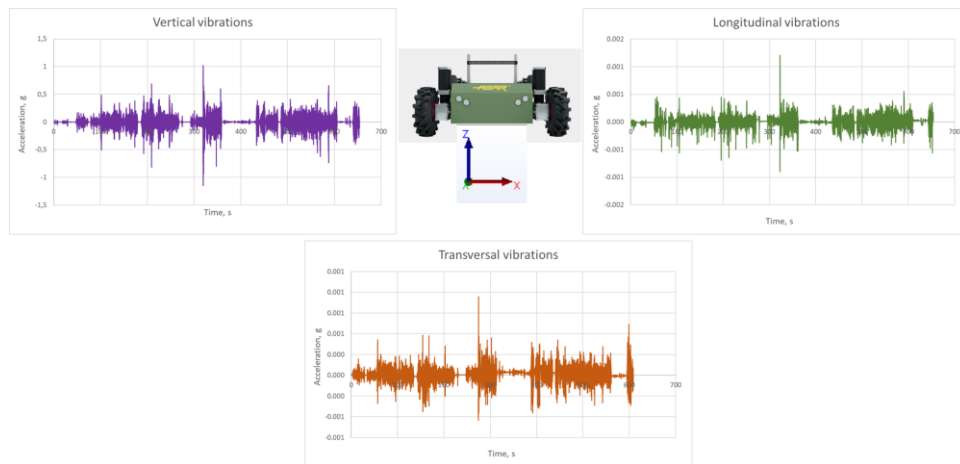
Fig. 7 Identification of worst-case load scenario by robot main body acceleration

In the second worst-case operational scenario it is determined that crossing the elevated static objects, such as rocks or curbs, along the movement path introduces an additional vibration load to the robot mechanical components. The movement over the rough terrain generates a lower vibration load than the crossing of elevated static objects; the contact of robot wheels with noted objects generates an impact which additionally stresses the mechanical components. The maximal vibration load during TRL6 prototype validation was observed while climbing the curb at full robot speed as shown on Figure 7. The vibration load is the largest in the vertical direction and significantly lower in lateral and longitudinal directions. As the vertical vibrations are two orders of magnitude larger than

the lateral and longitudinal vibrations, the latter two were neglected in further analysis. The maximal acceleration in the vertical direction is 2.1 g, as shown in Figure 7.

The method used to lightweight the robot mechanical components consists of a sequential combination of the static structural analysis by the finite element method followed by the topology optimization. The analysis was performed in Ansys Workbench 19.2 software package.

The static analysis was used to calculate the effects of static loading of the mechanical components of the robot, while an inertial force of gravity was also considered. The static structural analysis is divided into two load cases:

- first analysis (load case 1) is the analysis of the structural integrity of the robot mechanical components due to the "tank" rotation during the change of the direction of moment, while considering the friction between the wheels and the surface base. In the noted load case it is considered that one of the wheels is fixed, as it introduces the maximal load for the robot mechanical components;
- second analysis (load case 2) is the analysis of the robot mechanical components structural integrity for the second worst-case operational scenario i.e. due to the vertical acceleration load of 2.1 g.

The results of the static structural analysis were then used in the topology optimization analysis with a goal to identify which geometry volumes which can be removed to reduce mass of the robot mechanical components. Based on results of topology optimization, as well as strain energy distribution determined in the static structural analysis, the 3D model of the robot was revised to reduce the mass. The new static structural analysis was then performed with a revised 3D robot geometry to ensure that the revised design has satisfactory strength and stiffness.

4. STATIC STRUCTURAL ANALYSIS

For this analysis purposes geometrical model of the robot are simplified in order to reduce time and resources needed for the analysis without tradeoffs in simulation accuracy. The linear electric actuators were replaced by a steel rod which is locking the clearance adjustment mechanism at the lowest position, as the noted position was identified as a worst-case load in load case 1. Fasteners were removed from the analysis as they do not contribute significantly to the robot stiffness. The pneumatic tires were replaced with a simplified geometry and it was considered that they were made from ABS plastics as their stresses and deformations were not a subject of static structural analysis. The simplified geometric model of the robot can be seen in Figure 8.

Materials which are used in robot design were:

- Aluminum alloy 6061 for all main body profile components,
- structural steel S355 J2GR for the main body enclosure and reinforcements, components of the clearance change mechanism and wheel hub and rim,
- steel C45 for shafts, pins and spacers, and
- ABS plastics for tires, as the pneumatic tires were replaced by ABS plastics for analysis purposes.
- Table 1 defines the mechanical characteristics of the materials used in the analysis.
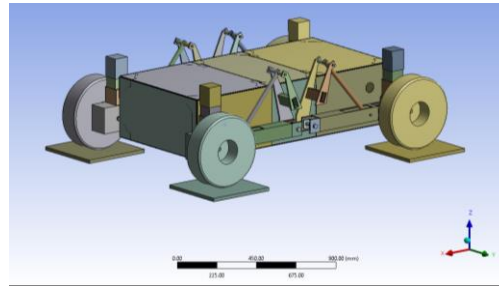
Fig. 8 Simplified geometrical model of the robot

Table 1 Material properties

Aluminium Alloy 6061	Value	Structural Steel S355 J2GR	Value
Tensile Yield Strength	259 MPa	Tensile Yield Strength	355 MPa
Tensile Ultimate Strength	313 MPa	Tensile Ultimate Strength	510 MPa
Density	2710 kg/m3	Density	7850 kg/m3
Young's Modulus	68300 MPa	Young's Modulus	200000 MPa
Poisson's Ratio	0.33	Poisson's Ratio	0.3
Structural Steel C45E	Value	ABS plastics	Value
Tensile Yield Strength	490 MPa	Tensile Yield Strength	41.4 MPa
Tensile Ultimate Strength	700 MPa	Tensile Ultimate Strength	44.3 MPa
Density	7850 kg/m3	Density	1040 kg/m3
Young's Modulus	200000 MPa	Young's Modulus	2390 MPa
Poisson's Ratio	0.3	Poisson's Ratio	0.399

Meshing was performed with 3D [17] higher order elements to exactly capture the geometry of some of the design elements, as well to increase the accuracy of simulations. Maximum mesh skewness of the model was below 0.85 which satisfy the mesh quality criterion and thus provides confidence in simulation results. The model consists of 1178893 nodes which form 328824 finite elements. A mesh size sensitivity test was performed to obtain confidence in accuracy of finite element simulations. It was assumed that the simulation results are insensitive to the mesh size if the difference in equivalent stress and total deformation in two adjunct meshes is below 3%. The model finite element mesh is shown on Figure 9. Face sizing was done on the contact surfaces where the frictional contact between the elements exists.
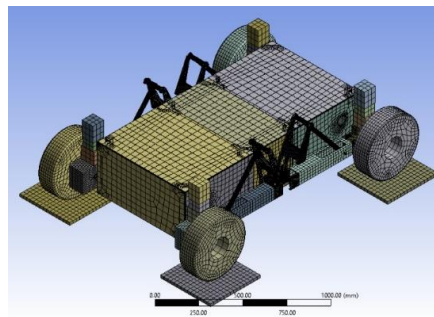

Fig. 9 FEM mesh of the AgAR robot

Figure 10 shows the loads and boundary conditions for the two worst-case load scenario – "tank" turning with one wheel fixed (Load case 1) and increased load due to vertical vibrations (Load case 2). In both load cases, the battery weight (600 N) and robot payload (3000 N) were introduced as force loads acting on corresponding surfaces.

a)   b)
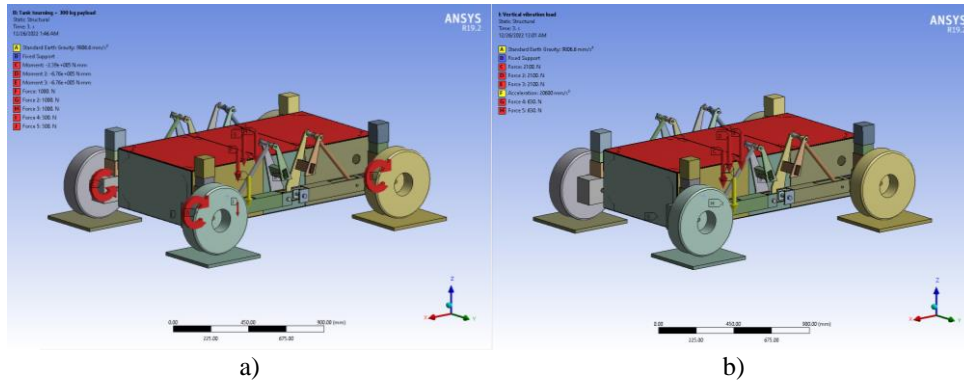
Fig. 10 Boundary conditions and loads for Load case 1 (a) and Load case 2 (b)

For the Load case 1, the friction coefficient is considered as 0.6 for the contact of wheels with the ground.

The performed static structural analysis showed that the maximal stresses and deformations occur for the Load case 1. The analysis showed that the robot chassis has a good structural integrity. The maximum equivalent stress (Figure 11) occurs on the connecting rod pivot pin and it amounts to approximately 320 MPa which is bellow the yield strength of the material of the pivot pins (steel C45E).
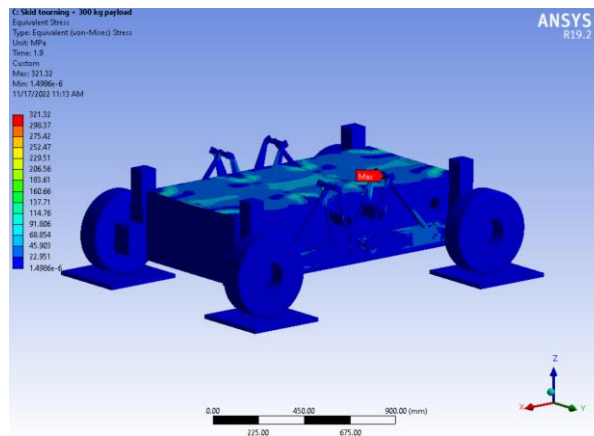

Fig. 11 Stress distribution of robot mechanical components for Load case 1

5. TOPOLOGY OPTIMIZATION

Topology optimization was performed for the critical load case – Load case 1, where equivalent stresses had the highest values. The first step in the topology optimization was to

define an optimization region i.e. the 3D region where the change of material layout is possible. All surfaces where loads or boundary conditions were applied were excluded from the optimization region. Furthermore, all other functional surfaces were also excluded from the optimization region. The second step in the topology optimization procedure was to define an optimization goal. As already noted, the primary goal of the study was to decrease the mass of the AgAR mechanical components, so a 20% reduction of mass was adopted as a goal of analysis. The results of topology optimization are shown in Figure 12.
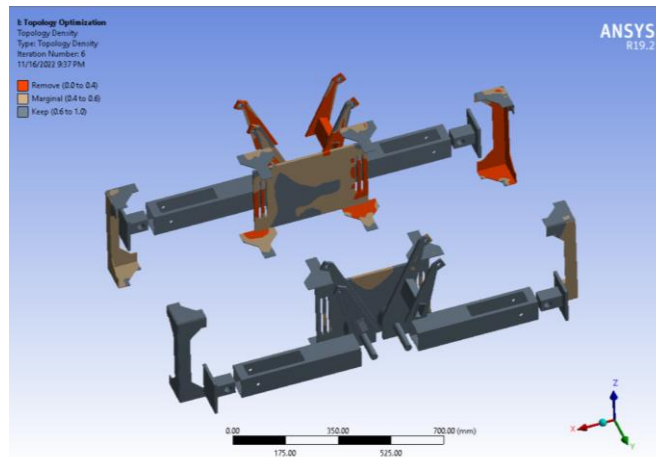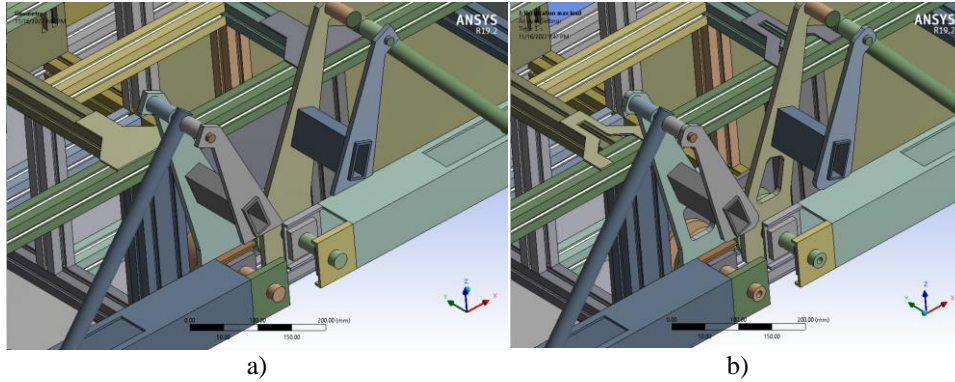

Fig. 12 Results of topology optimization for Load case 1

Based on results of the topology optimization a redesign of AgAR robot was performed, keeping in mind that during operation the robot can rotate around the vertical axis in tank turning on both sides – clockwise and counterclockwise. The redesign was performed also in respect to results of the strain energy distribution for Load case 1 shown on Figure 13.
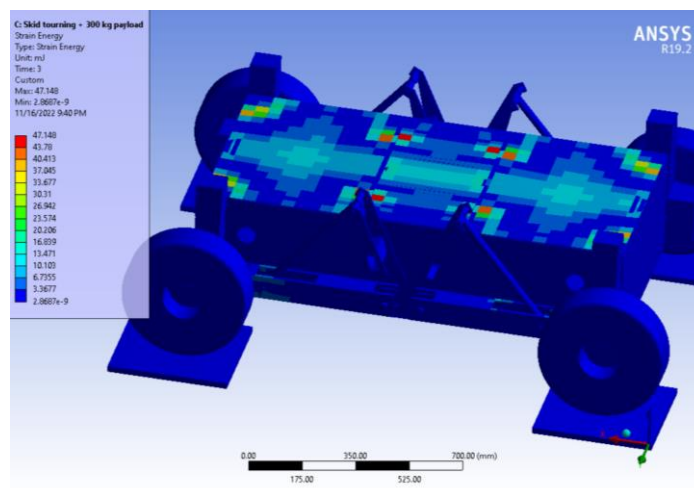

Fig. 13 Strain energy distribution for Load case 1

Figure 14 shows the comparison of the preliminary and new 3D design of robot mechanical components. The redesigned AgAR mechanical components mass is 285 kg which is a reduction of approximately 17% compared to the starting robot mass of 340 kg.

a)	b)

Fig. 14 Results of topology optimization for Load case 1

The structural analysis was again performed for a redesigned robot for a Load case 1 in order to perform the verification of the new design. Figure 15 shows the results of stress distribution of the redesigned AgAR mechanical components. The maximum equivalent stress again occurs on the connecting rod pivot pin, and it is increased to 345 MPa. Although the maximal stress is increased, it is bellow the yield strength of the steel C45E as the material of the pivot pins.
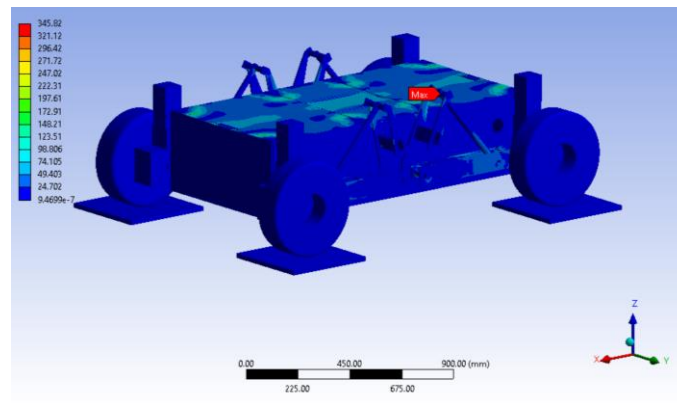
Fig. 15 Stress distribution of the redesigned robot mechanical components for Load case 1

7. CONCLUSION

The paper presents the case study of the robot UGV lightweighting based on digital twin data about operational loads. The process of creation of the robot UGV digital twin is described, as well as the identification of the worst-case operational load cases. The

static structural analysis and topology optimization were performed for the worst-case operational load.

Based on the obtained results, it can be concluded that digital twin data can be successfully used to optimize the robot UGV. By application of real-world operational load data, the mass reduction of approximately 17 % was achieved. The future direction of research would be directed towards the further optimization of the AgAR design with a goal of mass reduction by material substitution and using sheet metal parts to substitute the parts made by machining. Furthermore, the AgAR digital twin will be progressed to higher maturity level with the inclusion of the Artificial Intelligence for maintenance and control purposes.

REFERENCES

[1] Henning, F., Moeller, E., Handbuch Leichtbau, Hanser Verlag, (2011).

[2] M. Banić, M. Perić, L. Stojanović, Structural Analysis of Robot for Train Undercarriage Visual Inspection, Proceedings of XX Scientific-Expert Conference on Railways RAILCON '22, 978-86-6055-160-5, Niš, Serbia, 13. - 14. Oct, 2022, pp. 21 – 24.

[3] M. Banić, M. Simonović, L. Stojanović, D. Rangelov, A. Miltenović, M. Perić, Digital Twin-Based Unmanned Outdoor Field Robots Lightweighting, XVI International Conference SAUM 2022, 978-86-6125-258-7, Niš, Serbia, 17. - 18. Nov, 2022, pp. 9 – 14.

[4] M. Mikell, Immersive analytics: the reality of IoT and digital twin, IBM Business Operations Blog, (2017).

[5] M. Crawford, 7 Digital Twin Applications for Manufacturing, ASME, (2021).

[6] C. Miskinis, The history and creation of the digital twin concept, Challenge Advisory, (2019).

[7] Lockheed Martin Corporation, Visualizing the Digital Thread = Digital Twins at Lockheed Martin, (2021).

[8] R. Goraj, Digital twin of the rotor-shaft of a lightweight electric motor during aerobatics loads, Aircraft Engineering and Aerospace Technology, 92(9), 2020, pp.1319-1326.

[9] P. Kokkonen, B. Hemming, E. Mikkola, J. Junttila, V. Lämsä, Robust lightweight design and digital twins considering manufacturing quality variation and sustainability requirements, XIV Finnish Mechanics Days 2022, May 18–20, 2022, Lappeenranta, Finland

[10] T. Ryll, M. Kuhtz, L. Quirin, M. Nguyen, M. Gude, A. Filippatos, Design approach for the development of a digital twin of a generic hybrid lightweight structure, MATEC Web of Conference 349, 03004 (2021), ttps://doi.org/10.1051/matecconf /202134903004

[11] J. Rupfle, C.U. Grosse, Soft real-time framework for Structural Health Monitoring of wind turbine supporting structures, International Conference on NDE 4.0 – 2022

[12] Zhang, X.; Zhang, X.; Zhang, M.; Sun, L.; Li, M. Optimization Design and Flexible Detection Method of Wall-Climbing Robot System with Multiple Sensors Integration for Magnetic Particle Testing. Sensors 2020, 20, 4582. https://doi.org/10.3390/s20164582

[13] Laukotka, F.; Seiler, F.; Krause, D.: MBSE als Datenbasis zur Unterstützung von Konfiguratoren und Digitalen Zwillingen modularer Produktfamilien, Proceedings of the 31th Symposium Design for X (DFX2020), Bamberg, Germany, 2020, pp. 61-70. DOI: 10.35199/dfx2020.7

[14] Tuegel, E.J.: The Airframe Digital Twin: Some Challenges to Realization, 53rd AIAA/ASME/ASCE/ AHS/ASC Struct. Struct. Dyn. Mater. Conf, pp. 1812, 2012. DOI: 10.2514/6.2012-1812

[15] Laukotka, F.; Hanna, M.; Schwede, L.-N.; Krause, D.: Lebensphasen-übergreifende Nutzung Digitaler Zwillinge – Modellbasierte Produktfamilienentwicklung am Beispiel der Flugzeugkabine, Zeitschrift für wirtschaftlichen Fabrikbetrieb (ZWF), Vol. 115, 2020, pp. 101-104. DOI: 10.3139/104.112332

[16] Herlitzius, T. How Much Lightweight Design Does Agricultural Technology Need?. ATZ Heavy Duty worldw 15, 54 (2022). https://doi.org/10.1007/s41321-021-0466-7

[17] ANSYS Release 19.2 documentation, (2020).